Lift-Off Acoustics Predictions for the Ares I Launch Pad

Kenneth J. Plotkin, Wyle Laboratories
Louis C. Sutherland, LCS Acoustics
Bruce T. Vu, NASA Kennedy Space Center

1.0 Introduction

The vibroacoustic environment associated with large launch vehicles is of concern for the integrity of the launch complex and the vehicle itself. A large body of knowledge of this environment was developed during the early years of the missile and space flight, particularly during the Apollo program. Reference 1, prepared by Sutherland and others during that era, contains much of that knowledge. A specific process for predicting noise on and around the vehicle itself and the launcher is presented in Reference 2, prepared by Eldred, et al. Recent reviews of the process, e.g., Reference 3, have suggested some revised details but generally support the methodology in Reference 2.

Figure 1 is a sketch of the procedure defined in Reference 2 for predicting the acoustic environment on a launch vehicle while in the vicinity of the pad. The rocket exhaust plume is represented at a distribution of acoustic sources along its centerline, as turned by the deflector. The model consists of the following overall elements:

1. The overall sound power level emitted by a rocket
2. The spatial distribution of the sources as a function of distance along the plume
3. The spectral content and directivity of the sources, again as a function of distance along the plume

Each of these elements was derived in scalable form from available measured noise data, some from model experiments and some from actual launches. While Figure 1 is sketched as a prediction of noise on the vehicle itself, it is applicable to the launch pad and tower structure.

Figure 2 is a generalization of this modeling approach, showing the deck and tower of a modern Mobile Launcher, with noise along the tower being of interest. A detail of this configuration is that the deck itself blocks the propagation path from part of the plume.

In the time since Reference 2 was published, there has been considerable research in jet and rocket noise modeling and sound propagation. For example, the overall sound power model in Reference 2 is based on a simple acoustic efficiency factor, and is not consistent with Lighthill's well established jet noise theory.[4,5] Consistent rocket noise models are now available, as is research on source distributions and characteristics as well as a much better understanding of the shielding of noise by parts of the launcher itself.

A new model, denoted PAD,[6] has been prepared for application to the Ares I vehicle and its mobile launcher. The geometry modeled is that sketched in Figure 2 for the vehicle on the pad, and Figure 3 for the vehicle at some height above the pad. The components of the model are described in Section 2.

2.0 Model components

2.1 Overall Sound Level

The overall acoustic sound power W_a radiated by a rocket has often been considered to be a fraction of the mechanical power W_m of the jet, i.e.,

$$W_a = \eta W_m \tag{1}$$

where η is an acoustic efficiency factor. Data summarized in Reference 2 fit this relation well, with η varying from 0.5% to 1.0%. The fits do not provide a method to assess η for a particular rocket, and the form of Equation 1 is not consistent with Lighthill's jet noise theory.[4,5]

Sutherland[7,8] introduced the factor G

$$G = (\gamma/\gamma_0)(c_e/c_0)^3(c_e/V_e)^2 \tag{2}$$

where

V_e = flow velocity at nozzle exit
c_0 = ambient sound speed
c_e = sound speed at the tip of the supersonic core
γ_0 = ratio of specific heats in the atmosphere
γ_e = ratio of specific heats at the tip of the supersonic core

such that Equation (1) may be written as

$$W_a = KGW_m \tag{3}$$

where K is a constant determined by a fit to the experimental data. Figure 3, from Reference 7, shows the best fit to data summarized in References 2 and 5. This result is much tighter than fits according to Equation (1), and an efficiency does not have to be estimated. Expressed as a sound power level, the fit is

$$L_W = 93.1 + 10\log_{10}(GW_m) \text{ , dB re: 1 picowatt} \tag{4}$$

where K and the scale factor relative to the reference sound power level are contained in the leading constant of 93.1 dB.

2.2. Source Distribution and Directivity

Noise sources are distributed along the jet axis according to the following relation, which is a fit to the distribution in Figure 12 of Reference 2

$$W(x)/W_a = 0.312\left(\frac{x}{x_t}\right)^{1.36} \Bigg/ \left[1 + .005908\left(\frac{x}{x_t}\right)^{7.745}\right]^{0.9091} \qquad (5)$$

where x is axial distance from the nozzle exit plane, $W(x)$ is the acoustic power density per unit length, and x_t is the core length. Based on data in References 4 and 9, the following relation has been used in a number of places, including Reference 2

$$\frac{x_t}{d_e} = 3.45(1 + 0.38M_e)^2 \qquad (6)$$

where d_e is the nozzle exit diameter and M_e is the exit Mach number. This relation has come into question, and it is apparently based on jets that are pressure matched to the ambient. More recent literature suggests that x_t is considerably shorter for non-matched exit conditions. Sample calculations in Reference 2 for a solid rocket with parameters similar to the Shuttle-SRM-based Ares I suggest a core length about 40% that given by Equation (6). An improved x_t relation, including the effect of exit pressure ratio, is being developed. As an interim step, a multiplier of 0.4 is being used for Ares I predictions.

2.3. Spectra and Directivity

The noise source spectrum at each axial distance is scaled from the normalized spectrum shown in Figure 4, taken from Reference 2. The directivity is based on an updated analysis of data, shown in Figure 5. Analytic curve fit relations were developed for both spectrum and directivity.

3.0 Modeling

3.1 Geometry

The geometry was modeled as sketched in Figure 1. Coordinates are X positive from the center of the flame hole, and Z positive above the deck. Key elements are:

- Launcher deck, with opening for plume, at height Zdeck;
- Deflector, with top at height Zdefl;
- Trench, with top at height Zdefl and bottom at Zbot;
- Vehicle above the flame hole, nozzle exit plane at height Z0 (= Zdeck in Figure 1).

The exhaust plume is presumed to have the same properties as an undeflected plume, but its centerline is defined by:

- Straight (vertical) from Z0 to Zdefl;
- Circular arc past the deflector, at radius Rdefl = (Zdefl-Zbot)/2. This assumes the plume fills the trench;
- Straight exit, at a final turning angle.

3.2 Sound Propagation

The noise sources along the exhaust plume are as defined in Section 2.0. Each source element radiates sound that propagates to receiver points by geometrical spreading. For free space, geometric spreading is spherical and there is a $4\pi r^2$ dependence. As described in Reference 1, for a source on the ground the sound radiation is hemispherical and there would be a $2\pi r^2$ dependence. For a source at h above the ground, and distances $r > h$, there is an intermediate behavior given by $2\pi(r+h)r$. Note that at $r = h$ this matches spherical spreading. In the model, geometric spreading is governed by $2\pi(r+h)r$ for $r > h$ and $4\pi r^2$ for $r < h$.

As sketched in Figure 1, paths from some parts of the plume are blocked by the deck. Shielding is computed via Maekawa's thin screen model.[10]

Noise impinging on the launcher, vehicle and top of the deck is computed. Noise underneath the deck is not computed. Predicted noise levels are free field, i.e., reflections from the launcher or vehicle, or local doubling on solid surfaces, are not applied within the program, but are readily applied when using program output for analysis.

Air absorption is small for the distances of interest, and is not included.

4.0 Implementation

The process described above was implemented in software. Based on vehicle and launcher parameters specified by the user, it computes overall sound pressure level and spectra on a grid of points in X, Z coordinates. For the currently planned Ares I launch configuration, the vehicle, tower and flame trench are all in a line, so a 2-D output grid is sufficient. The software is currently being expanded to allow full 3-D geometry. That expansion consists of adding the Y coordinate, and generalizing the shielding algorithms which exploited the simplicity of the 2-D geometry.

The software was prepared as two modules. The first is a computational module that runs in batch mode, yielding predicted spectra at the grid locations for each vehicle height. This is written in standard Fortran 90, and is not machine dependent. Results are in a simple tabular format, which are straightforward to read or to load into other software for further analysis. The second module is a display, and uses a PC-specific graphics library. Figure 6 shows a typical display result. The primary display is the spectrum at the selected receiver. There are two lines of annotation in the upper right corner. The first shows the receiver position (X, Z) and the OASPL. The second shows the vehicle height Z0, the height of the exhaust plane above the launcher deck.

There is a sketch in the lower left that shows the launcher, the vehicle, the plume shape, and the OASPL contours. There is a circle marking the receiver X, Z position. The user can move the receiver point around on the grid via the cursor keys. If a full run is performed, with multiple vehicle heights, the user can view results at various heights.

5.0 Summary

A model has been developed to predict the launch noise environment for the Ares I. It is based on the general methodology of Reference 2. It contains improved source modeling details developed in more recent years. It accounts for launch pad and deflector geometry, including shielding by the launcher deck. It has been implemented in a Fortran package, with a display module for interactive viewing of results.

References

1. Sutherland, L.C. (ed.), "Sonic and Vibration Environments for Ground Facilities - A Design Manual." Wyle Laboratories Report WR 68-2, 1968.

2.Eldred, K. McK., et al, "Acoustic loads generated by the propulsion system." NASA Space Vehicle Design Criteria (Structures), NASA SP-8072, June 1971.

3. Varnier, J., et al, "Noise radiated from free and impinging hot supersonic jets." AIAA-98-2206.

4. Lighthill, M.J., "Sound Generated Aerodynamically," The Bakerian Lecture 1961, Proc. Royal Soc. (London), A267, 1962, pp 147-182

5. Lighthill, M.J., "Jet Noise," AIAA Journal, Vol. 1, No. 7, July 1963, pp 1507-1517

6. Plotkin, K.J. and Sutherland, L.C., "Prediction of the Acoustics Environments Induced by the Launch of the Ares I Vehicle," Wyle Report WR 07-27, December 2007.

7. Sutherland, L. C., "Progress and problems in rocket noise prediction for ground facilities", AIAA-93-4383, Presented at 13th AIAA Aeroacoustics Conference, Long Beach, Ca. Oct. 25-27, 1993.

8. Sutherland, L. C., “A rocket noise source model for prediction of ground environments near launch sites”, Consulting Report 96-1, Apr. 1996.

9. Anderson, A.R., and Johns, F.R., "Characteristics of Free Supersonic Jet Exhausting into Quiescent Air," Jet Propulsion, Vol 25, No. 1, Jan 1955, pp 13-15

10. Maekawa, Z., "Noise Reduction by Screens." Applied Acoustics, Vol. 1, pp 157-173, 1968.

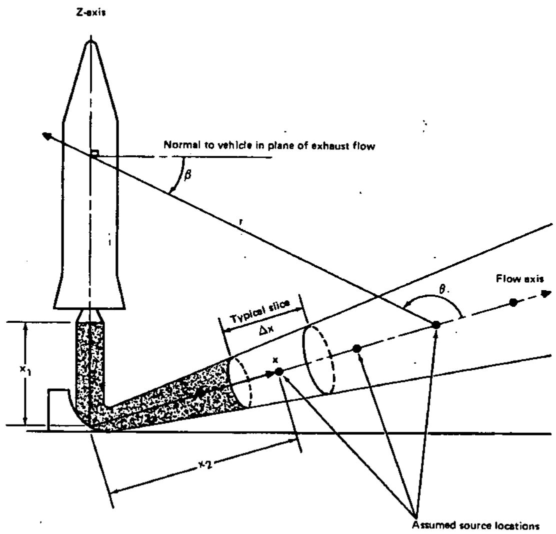

Figure 1. Modeling of noise on launch vehicle, from, NASA SP-8072

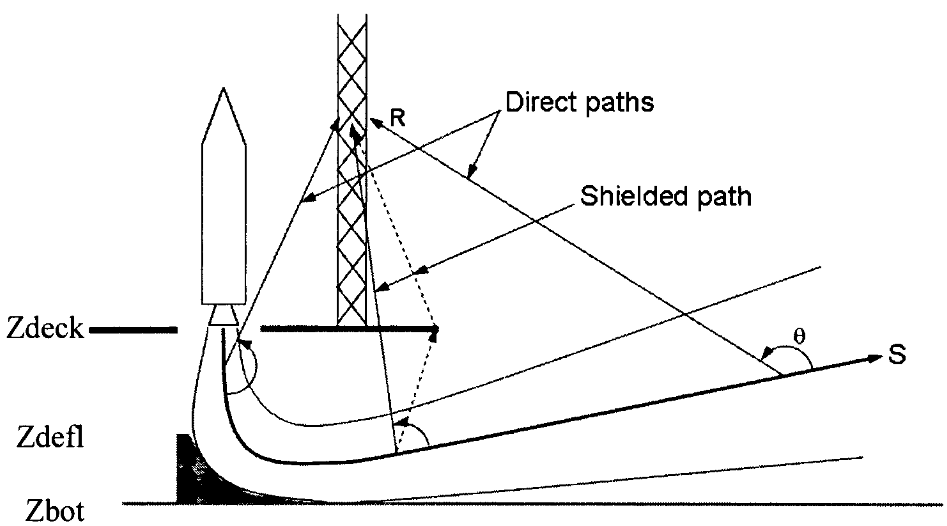

Figure 2. Launch Pad representation for modeling

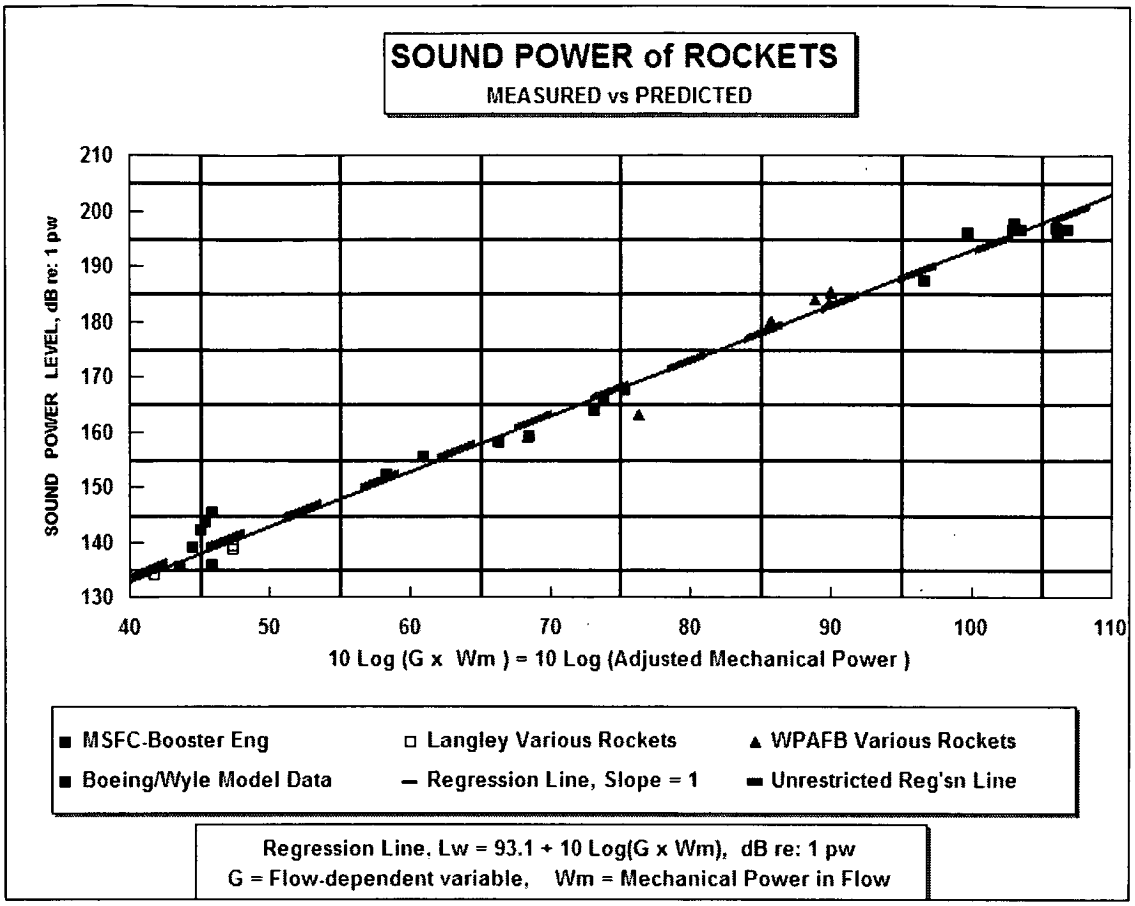

Figure 3. Fit of predicted sound power versus mechanical power for rocket engines

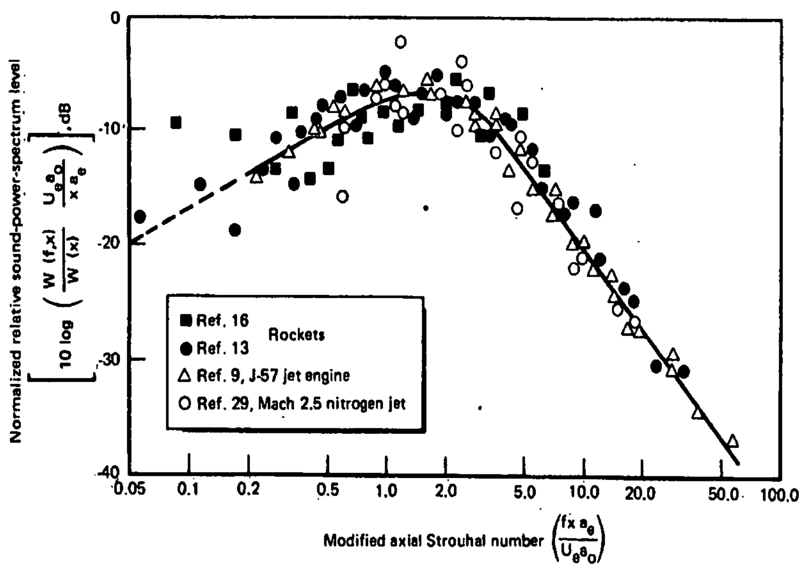

Figure 4. Normalized spectrum for rocket noise, from Reference 2

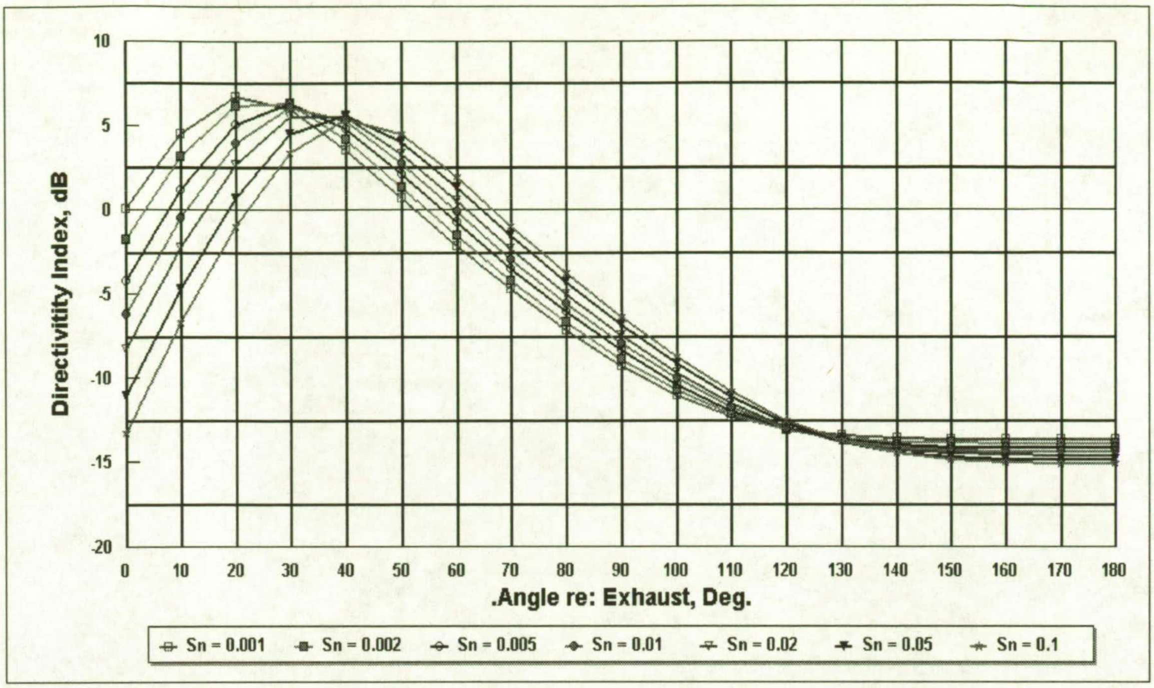

Figure 5. Directivity index as a function of Strouhal number

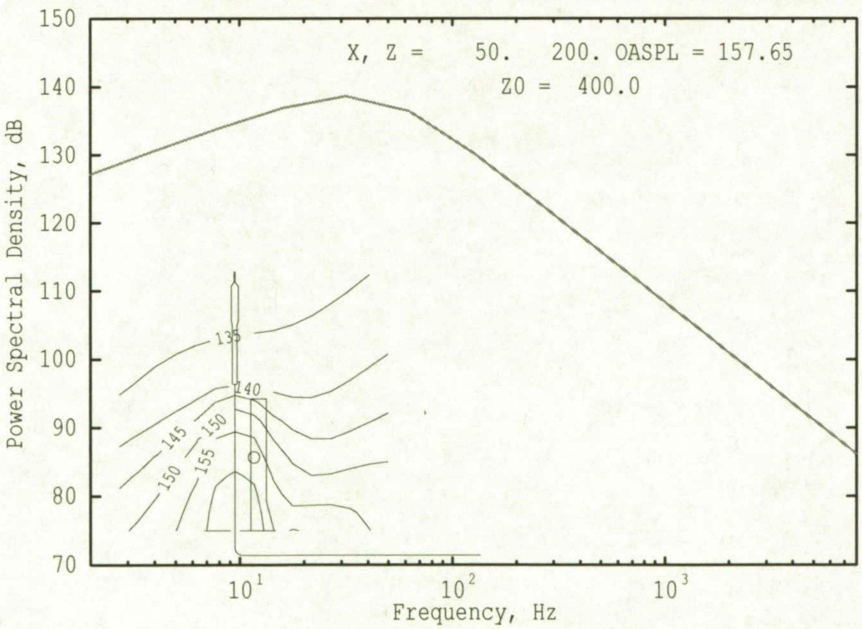

Figure 6. Typical display of results, vehicle 400 feet above deck